Mitigating Non-CO_2 greenhouse gases in an integrated assessment model

Dominique van der Mensbrugghe[1] and Maksym Chepeliev

April 15, 2021

Abstract: This paper has two purposes. First, it incorporates one method for mitigating non-CO_2 emissions in a computable general equilibrium (CGE) model. Mitigation of combustion-based CO_2 emissions is a relatively straightforward exercise and has been implemented in many models. Non-CO_2 emissions are driven by a number of factors and their mitigation relies on complex set of technologies. These have been approximated by so-called marginal abatement cost curves, which represent a reduced-form relation between the price of emissions and their percent reduction. Second, the paper illustrates how to readily convert a CGE model into an integrated assessment model (IAM) that links economic-based emissions to a temperature signal using a simple climate model. Subsequently, the temperature signal is linked to changes in one or more economic drivers such as crop yields or labor productivity. Both enhancements allow for more detailed modeling of the economics of climate change.

JEL Codes: ¿¿¿¿ INSERT JEL CODES HERE ¡¡¡¡
Keywords: ¿¿¿¿ INSERT KEYWORDS HERE ¡¡¡¡

[1] The Center for Global Trade Analysis, Purdue University, 403 West State Street, West Lafayette, IN 47906. Corresponding e-mail: vandermd@purdue.edu.

Contents

List of Tables

List of Figures

Chapter 1

Introduction

As countries have started implementing their Nationally Determined Contributions (NDCs) in the context of their commitments to the 2015 Paris Agreement that aims to limit the global mean temperature rise to at most 2°C and preferably to 1.5°C, they are looking at a wide range of instruments to mitigate emissions of greenhouse gases (GHG). Much of the traditional focus is the taxing of carbon—mostly linked to combustion of fossil fuels. It has been postulated that cheaper options could be available that rely on other sources of greenhouse gas emissions such as methane in agriculture (rice production, livestock and dairy), resource extraction and waste management, and nitrous oxide emissions in agriculture, chemical production and waste management.[1]

This paper:

- reviews the existing literature on multi-gas mitigation
- discusses an updated version of GTAP's non-CO_2 emissions database that differentiates the emission drivers between combustion of fossil fuel and other processes, further extending the latest GTAP 10 non-CO_2 emissions database
- describes implementation of non-CO_2 emissions in a GTAP-based integrated assessment model (IAM)
- describes the calibration of the non-CO_2 marginal abatement cost (MAC) curves to the most recent estimates of these curves developed by the U.S. Environmental Protection Agency (U.S. EPA (2019))
- illustrates the impacts of including non-CO_2 mitigation using interpretations of the NDCs and more stringent mitigation targets consistent with the 2°C efforts

The non-CO_2 emissions database, corresponding MAC curves and climate model developed in this paper can be easily incorporated to GTAP-based CGE models, thus allowing for a more consistent assessment of the climate mitigation measures.

In addition to the focus on non-CO_2 mitigation, the paper will also describe implementation of a new climate module. One particular feature of the most IAMs is their linkage to a simple climate model—most famously Nordhaus' DICE model (Nordhaus (2016)). Modelers have two options in coupling to a simple climate model. One alternative, used by many models, is to link to an external simple climate model—such as the MAGICC model (Meinshausen et al. (2011)), or HECTOR (Hartin et al. (2015)). This entails iterating between the IAM and MAGICC or

[1] See papers linked to the Energy Modeling Forum Study No. 21 (EMF-21) in Weyant et al. (2006).

HECTOR until (near) convergence is achieved. Emissions from the IAM are used as inputs to the simple climate model, which then evaluates the climate indicators, such as changes in mean global surface temperature. The latter are then used as inputs to evaluate the economic impacts—for example changes in crop productivity. A second alternative is to code the climate module directly into the IAM—the approach taken by DICE, as well as the MERGE model (Manne et al. (1995)). The MERGE model implementation explicitly allows for a multi-gas assessment, unlike DICE that only includes the carbon cycle with the impacts of other gases summarized by an exogenous shock to radiative forcing. The equations and their parameterization are readily available and provide easy implementation into a global CGE model. This approach absolves the need to iterate between the CGE and climate models and also allows for more direct implementation of specific targets, for example setting the temperature change not to exceed 2°C.

This paper will describe a relatively new simple climate model that is based on the FAIR model (Millar et al. (2017), Smith et al. (2018) and Leach et al. (2020)), as well as an implementation of the FAIR model by Hänsel et al. (2020). The focus will be on the most recent version of FAIR, FAIR 2.0 described in detail in Leach et al. (2020). This model includes a multi-gas assessment, a more realistic carbon cycle model that hones closer to the large climate models and a three-box temperature model that also provides a better approximation of the long-run temperature cycle. The original model has been coded in Python, but the equations are implemented in GAMS and incorporated into a global CGE model. The GAMS version has been thoroughly tested and reproduces exactly the results from the original Python version (for the same set of inputs). The paper discusses the structure of the climate module and the requirements to integrate it into most standard global CGE models.

Chapter 2

Integrating Non-CO_2 gases and MAC Curves

2.1 Specification

The standard way for dealing with mitigating GHG not linked to the combustion of fossil fuels is to aggregate them together into a greenhouse gas bundle and combine the GHG bundle with output in a top-level constant elasticity of substitution (CES) aggregation of the two, see figure 2.1. The share parameters and the CES elasticity (σ^{ghg}) are calibrated to observed MAC curves. Thus, if GHG are priced, the cost of the GHG bundle increases and producers substitute away from their use. The MAC curves link the price of GHGs to the decline in their use.

The GHG bundle itself is a CES composite of the underlying GHGs, the share parameters are calibrated to base year data. The other side of the production nest mimics the production technology of the standard underlying model. Depicted is the production nest of the GTAP model. The production nesting of the ENVISAGE model differs and also differentiates across crops, livestock and all other activities, (van der Mensbrugghe, 2019).

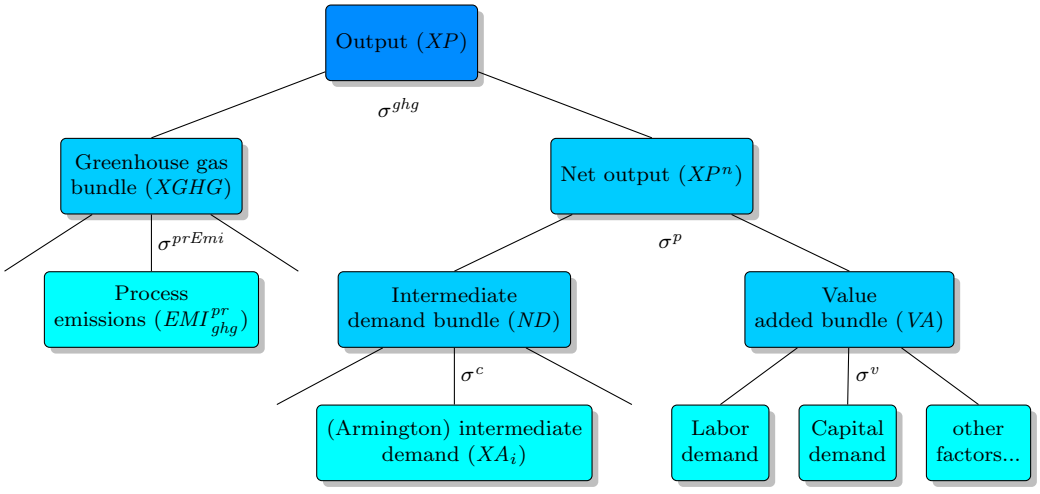

Figure 2.1: Production nesting with embedded greenhouse gases

2.2 Emissions data

The standard version of the GTAP Data Base coupled with the non-CO2 emission accounts includes four GHGs: carbon dioxide (CO_2), nitrous oxide (N_2O), methane (CH_4) and a composite bundle of fluorinated gases (FGAS). The first is linked exclusively to the combustion of fossil fuels (coal, crude and refined oil, natural gas). The other gases are linked to a set of three drivers: consumption of goods and services, production factors (such as land-based methane emissions in rice production, or herd-based (i.e. capital) methane emissions in livestock), and output (e.g. methane emissions from waste management).

In a new release of the emissions database (Chepeliev (2020) check citation) emission of greenhouse gases have been augmented to include so-called process emissions—some of which were already included in the original emission database such as factor- and output-based emissions. Consumption-based emissions are divided into two—those linked to the combustion of fossil fuels and those linked to process emissions. Figure 2.2 shows the global configuration of the GHG in 2014 divided into 7 production activities and final demand.[1] The levels are expressed in CO2 equivalent using the global warming potentials from the 4th Assessment Report (AR4) of the Intergovernmental Panel on Climate Change (IPCC). Emissions are color coded—red shades are linked to CO_2 emissions, green shades are linked to N_2O emissions, blue shades are linked to methane emissions and gold is linked to FGAS emissions. The brighest shades are linked to process emissions. The key findings from the chart include:

- Carbon dioxide emissions are the main source of total GHG emissions. Total emissions[2] amount to 46.6 gtCO2e, of which 64% are generated by the combustion of fossil fuels and 9% from CO_2 process emissions—a significant amount in the energy intensive sectors, notably cement production.
- Power generation is the largest source of emissions accounting for some 27% of total emissions.
- The bulk of N_2O, and CH_4 emissions are process emissions linked to agriculture, resource extraction, oil refining and services (mostly waste management).
- Non-fossil fuel combustion emissions represent some 34% of total GHG emissions.

2.3 The MAC curves

The MAC curves are provided by the U.S. Environmental Protection Agency (EPA). They reflect a mapping between carbon pricing and the percent reduction in emissions. Figure xxx provides an example for... The curves are used to calibrate the GHG gas bundle in the production nesting as reflected in figure 2.2.

2.4 Illustrative simulations

In this section, we map out model based MAC curves and with and without fossil fuel-based mitigation.

[1] Agriculture (AGR), extraction industries (XTR), oil refining (P_C), energy intensive activities (EIT), other manufacturing (XMN), electricity (ELY), services (SRV) and households (HHD).

[2] The emissions in the chart exclude emissions from land-use changes.

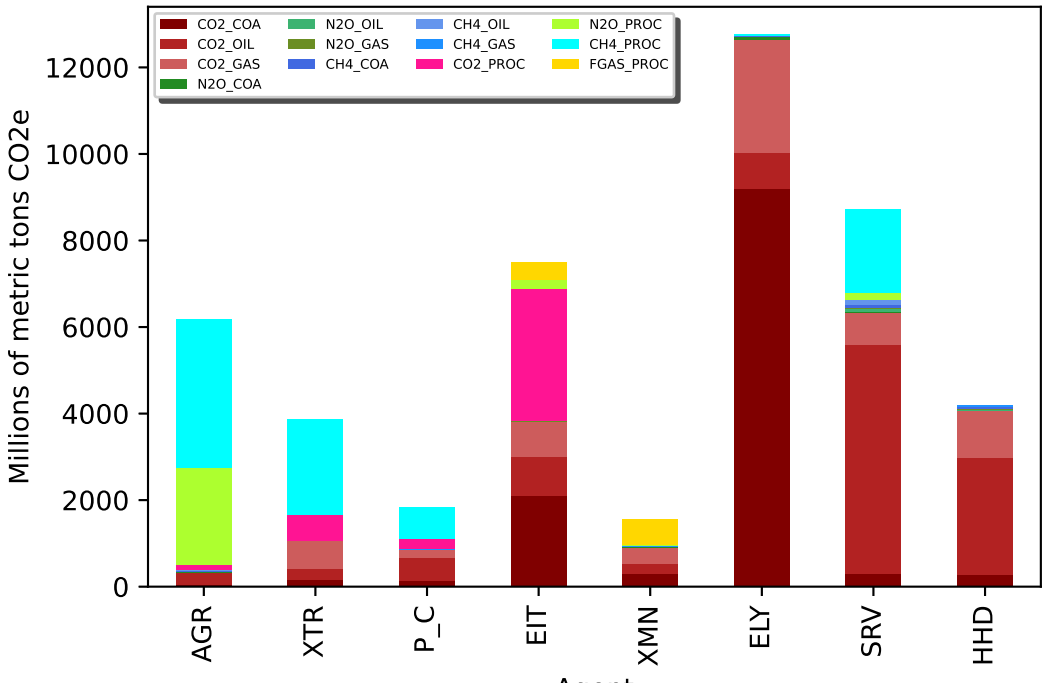

Figure 2.2: 2014 Global GHG Emissions

Chapter 3

From CGE to IAM

3.1 Introduction

An integrated assessment model (IAM) combines a socio-economic model with climate and impacts modules—see figure 3.1. The socio-economic model, such as a CGE, generates emission profiles driven by socio-economic drivers such as population and GDP growth, and assumptions about the emission generating process— the majority of which are driven by energy. The latter will be impacted by technological change, the energy mix, end-user preferences and policies. The IAM community is basing many of these assumptions using a family of scenarios called the Shared Socio-Economic Pathways (SSPs).[1] Emissions are ejected in the atmosphere and the carbon cycle module circulates carbon across the different carbon pools associated with the biosphere—the atmosphere, soils, and the oceans. The residual carbon in the atmosphere changes the radiative forcing, i.e. the amount of solar energy retained by the atmosphere. The final component, is the energy balance component that converts the change in radiative forcing to temperature change, which also involves different facets of the biosphere—notably the atmosphere and the oceans (possibly divided into the upper and deep oceans). Sophisticated climate models will generate other climate signals such as changes in precipitation. The IAM community is working with a family of four climate scenarios, known as representative concentration pathways. The final block completes an IAM cycle. Changes in climate will lead to changes in economic conditions—mostly negative—such as impacts on crop yields, labor productivity, water availability, etc.

Figure 3.1: Integrated assessment

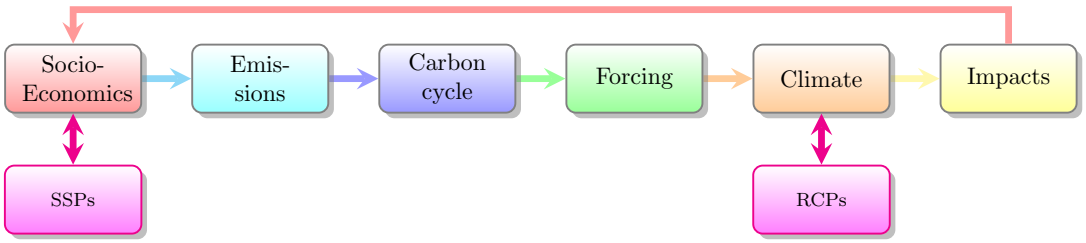

[1] See for example (O'Neill et al., 2015) and (Riahi et al., 2016).

3.2 A simple climate model

3.2.1 The carbon cycle

DICE

The most widely cited IAM model is Nordhaus' DICE model, the last version of which was made available in (Nordhaus, 2016). The DICE carbon cycle model relies on three boxes—atmosphere, upper ocean and lower ocean. The β parameters represent the fluxes between the boxes. Thus β_{11} represents the percent of carbon that remains in the atmosphere per period (88%) and β_{12} is the flux from the atmosphere to the upper ocean layer (12% of the atmospheric stock of carbon).[2] All CO_2 emissions are injected into the atmosphere and the remaining terms determine the fluxes across boxes. N.B. The β parameters must sum to 1 across a row.[3]

$$Conc_{atmos,t} = \beta_{11} Conc_{atmos,t-1} + \beta_{21} Conc_{upocn,t} + \frac{5}{3.666} Emi^{T}_{t-1} \tag{3.1}$$

$$Conc_{upocn,t} = \beta_{12} Conc_{atmos,t-1} + \beta_{22} Conc_{upocn,t-1} + \beta_{32} Conc_{dpocn,t-1} \tag{3.2}$$

$$Conc_{dpocn,t} = \beta_{23} Conc_{upocn,t-1} + \beta_{33} Conc_{dpocn,t-1} \tag{3.3}$$

FAIR

This section describes the main equations for the carbon cycle module developed for the Finite Amplitude Impulse Response (FAIR) model by Millar et al. (2017) and Smith et al. (2018) and reflects the latest incarnation in Leach et al. (2020) with some modifications. A variant was deployed in Hänsel et al. (2020) and replaced the DICE model's carbon cycle module using DICE's 5-year time step.

The FAIR model uses anthropogenic fossil and land use CO_2 emissions as input and partitions them into four boxes R_b—with partition fraction ϕ and τ representing the differing timescales of carbon uptake by geological processes (`1=GEOPR`), the deep ocean (`2=DPOCN`), the biosphere (`3=BIOSF`) and the ocean mixed layer (`4=MXOCN`). The equations represent an impulse response specification of the carbon cycle. The four 'reservoirs' represent different responses for the atmosphere summarizing the net fluxes of the true reservoirs on the atmosphere.

The motion equation for each box is given by equation (3.2.1). Some fraction φ of emissions finds its way into one of the four boxes.[4] Each box also is subject to decay with the τ parameter determining the rate of decay subject to an adjustment factor α. The adjustment factor α is a state dependent factor that depends on the level of CO_2 concentration. A discrete approximation for the differential equation is given in equation (3.4).

$$\frac{dR_{p,t}}{dt} = \varphi_p Emi_t - \frac{R_{p,t-1}}{\alpha_t \tau_p}$$

$$R_{p,t} = e^{-1/(\alpha_t \tau_p)} R_{p,t-1} + \alpha_t \tau_p \varphi_p Emi_t \left(1 - e^{-1/(\alpha_t \tau_p)}\right) \tag{3.4}$$

[2] The standard stepsize in DICE is 5 years.

[3] In the DICE model, carbon stocks in the three boxes are measured in gTC, thus emissions are multiplied by 12/44 to convert from CO_2 to C.

[4] The sum of the φ is 1.

State dependent decay adjustment factor

In the original version of the FAIR model, the α parameter is linked to two long-term conditions that refer to the integrated impulse response function (`iIRF100`), which represents the 100-year average airborne fraction of a pulse of CO_2 (Joos et al. (2013)).

The first of these conditions is the following:

$$iIRF100 = \sum_p \varphi_p \alpha \tau_p \left[1 - \exp\left(-\frac{100}{\alpha \tau_p}\right)\right]$$

This expression represents the explicit integrated impulse response function [TBC]. The second condition is:

$$iIRF100 = r^0 + r^C \left(CEmi_t - CEmi_t^n\right) + r^T Temp_t^{atm}$$

This expression proposed by Millar et al. (2017) is a simplified expression for `iIRF100` that depends on the total accumulated carbon in land and ocean sinks ($CEmi_{em} - CEmi_{em}^n$) and atmospheric temperature change $Temp^{atm}$ since the pre-industrial era. This increase in `iIRF100` and scaling of the time constants by α accounts for the land and ocean carbon sinks approaching saturation as more carbon is added to them (r^C parameter). In earth system models it is also observed that the efficiency of carbon sinks decreases with increasing temperature (r^T parameter).[5]

Setting the two expressions equal, we get an implicit equation for α:[6] The latest version of FAIR replaces the implicit expression with a numeric approximation that allows for an explicit expression for α.[7]

$$\sum_p \varphi_p \alpha \tau_p \left[1 - \exp\left(-\frac{100}{\alpha \tau_p}\right)\right] = r^0 + r^C \left(CEmi_t - CEmi_t^n\right) + r^T Temp_t^{atm} \tag{3.5}$$

The total impact on atmospheric concentration above pre-industrial levels is given by the sum across each of the boxes, equation (3.6). Total concentration including the pre-industrial level is given by equation (3.7).

$$Conc_{atmos,t}^n = \sum_p R_{p,t} \tag{3.6}$$

$$Conc_{atmos,t} = Conc_{atmos,t}^n + 588 \tag{3.7}$$

[TODO] Link the core carbon cycle model to this IR-style model.

In summary, both models yield $Conc_{atmos}$. The DICE version relies on an explicit representation of a simplified carbon cycle and yields carbon concentrations in three boxes: the atmosphere and upper and deep oceans. The FAIR model only yields atmospheric concentration based on an impulse response (IR) model that condenses a more complex carbon cycle involving interactions between various carbon sinks. In addition, it incorporates a state-dependent variable that modifies the behavior of the carbon cycle depending on current concentrations and the temperature change.

[5] In the latest version of FAIR, the expression is assumed to hold for methane as well with an added term reflecting α's dependence on actual concentration.

[6] FAIR 1.3 caps α at 100.

[7] See (Leach et al., 2020). Testing has shown that the two have very similar behavior, particularly as regards the impact on temperature (available from the author). Sharp deviations for the resulting α parameter only occurs for upper range values for emissions such as those in RCP8.5 in the later centuries.

3.2.2 Radiative forcing

The DICE and FAIR models use a similar specification for the radiative forcing component linked to carbon emissions, with a different parameterization, equation (3.8). The DICE version uses only the logarithmic component and the key parameter, ϕ^1, is equal to 3.6813. This represents the so-called climate sensitivity parameter and reflects the impact on radiative forcing from a doubling of CO_2 atmospheric concentration from its pre-industrial level ($Conc^{pi}_{atmos}$). The relevant climate sensitivity parameter for the FAIR model is 3.168.[8] However, in addition to the logarithmic component, the FAIR specification includes the square root component which adds to the logarithmic component. The value of the ϕ^3 parameter is 0.086.

$$Forc_t = \phi^1 \ln\left(\frac{Conc_{atmos,t}}{Conc^{pi}_{atmos,t}}\right) / \ln(2) + \phi^3 \left(\sqrt{Conc_{atmos,t}} - \sqrt{Conc^{pi}_{atmos,t}}\right) \tag{3.8}$$

Total radiative forcing is the sum of all components of radiative forcing. In the case of the full FAIR model, this includes some 60+ different impacts. In the DICE model, these are summarized in a single exogenous, though time-dependent, factor, equation (3.9).

$$RF_t = Forc_t + Forc^x_t \tag{3.9}$$

3.2.3 The Energy Balance Module

The energy balance module (EBM) mediates the changes in radiative forcing into a change in the global average atmospheric temperature change. This is represented as an impulse due to changes in RF and energy transfers between the atmosphere and the oceans. In the case of the DICE model, the oceans are represented by a single box. In the case of FAIR, the oceans are separated into upper and deep layers.

The EBM is based on a 3-box system using the following system of equations:

$$\dot{\mathbf{T}} = A\mathbf{T} + \mathbf{M}RF$$

where $\dot{\mathbf{T}}' = [\ \dot{T}_1 \quad \dot{T}_2 \quad \dot{T}_3\ ]$, $\mathbf{T}' = [\ T_1 \quad T_2 \quad T_3\ ]$, F is radiative forcing, $\mathbf{M}' = [\ 1/C_1 \quad 0 \quad 0\ ]$ and:

$$A = \begin{pmatrix} -(\lambda + \kappa_2)/C_1 & \kappa_2/C_1 & 0 \\ \kappa_2/C_2 & -(\kappa_2 + \varepsilon\kappa_3)/C_2 & \varepsilon\kappa_3/C_2 \\ 0 & \kappa_3/C_3 & -\kappa_3/C_3 \end{pmatrix}$$

The 'C' parameters represent the heat capacity of each of the boxes. The 'κ' parameters represent the heat exchange coefficients between the boxes. The 'λ' parameter is called the climate feedback parameter. And the 'ϵ' parameter is an efficacy factor that affects transient warming. In the case of DICE, κ^3 is 0 and the value of ϵ is irrelevant. Note as well that in the case of DICE, the parameterization is based on a 5-year time step. In the form given in equation (3.10), the change in atmospheric temperature can be solved as a difference equation, which also includes the temperature of the two ocean layers (or single layer in the case of the DICE model).[9]

$$\mathbf{Temp}_t = (I + A)\mathbf{Temp}_{t-1} + \mathbf{M}RF_t \tag{3.10}$$

[8] The FAIR model incorporates the '$ln(2)$' factor in the ϕ^1 parameter and hence its input value is 4.57.

[9] In the FAIR model, the EBM model is converted to an IR model that only solves for the change in atmospheric temperature. In essence, this involves diagonalizing the A matrix by calculating the eigenvalues and eigenvectors. Both the EBM and IR versions yield very similar results. Results available from the author.

In summary, carbon emissions from the CGE model are inputs into the carbon cycle module that change atmospheric concentrations. The latter impact radiative forcing which end up changing the energy balances as reflected in changes in atmospheric temperature. The next step converts changes in atmospheric temperature into bio-physical impacts such as changes in crop yields, labor productivity, and other impacts. The entire system is composed of only 7 equations in its simplest expression—that largely abstracts from other emissions and other drivers of changes in radiative forcing.

3.3 Damage module

3.4 Illustrative simulations

Chapter 4

Next steps

Appendix A

Tables

Appendix B

Standard GTAP sets for Version 10A

Table B.1: Regional dimension of the GTAP database

	Code	*Description*
1	AUS	**Australia**
2	NZL	**New Zealand**
3	XOC	**Rest of Oceania**
		American Samoa (asm), Cook Islands (cok), Fiji (fji), French Polynesia (pyf), Guam (gum), Kiribati (kir), Marshall Islands (mhl), Federated States of Micronesia (fsm), Nauru (nau), New Caledonia (ncl), Norfolk Island (nfk), Northern Mariana Islands (mnp), Niue (niu), Palau (plw), Papua New Guinea (png), Samoa (wsm), Solomon Islands (slb), Tokelau (tkl), Tonga (ton), Tuvalu (tuv), Vanuatu (vut), Wallis and Futura Islands (wlf)
4	CHN	**China**
5	HKG	**Hong Kong (China)**
6	JPN	**Japan**
7	KOR	**Republic of Korea**
8	MNG	**Mongolia**
9	TWN	**Taiwan (China)**
10	XEA	**Rest of East Asia**
		Macao (mac), North Korea (prk)
12	KHM	**Cambodia**
13	IDN	**Indonesia**
14	LAO	**Lao, PDR**
15	MYS	**Malaysia**
16	PHL	**Philippines**
17	SGP	**Singapore**
18	THA	**Thailand**
19	VNM	**Vietnam**
20	XSE	**Rest of Southeast Asia**
		Myanmar (mmr), Timor-Leste (tmp)

Table B.2: Regional dimension of the GTAP database (cont.)

21	BGD	**Bangladesh**
22	IND	**India**
23	LKA	**Sri Lanka**
24	NPL	**Nepal**
25	PAK	**Pakistan**
26	XSA	**Rest of South Asia**
		Afghanistan (afg), Bhutan (btn), Maldives (mdv)
27	CAN	**Canada**
28	USA	**United States**
29	MEX	**Mexico**
30	XNA	**Rest of North America**
		Bermuda (bmu), Greenland (grl), Saint Pierre & Miquelon (spm)
31	ARG	**Argentina**
32	BOL	**Bolivia**
33	BRA	**Brazil**
34	CHL	**Chile**
35	COL	**Colombia**
36	ECU	**Ecuador**
37	PRY	**Paraguay**
38	PER	**Peru**
39	URY	**Uruguay**
40	VEN	**Venezuela, Republica Bolivariana de**
41	XSM	**Rest of South America**
		Falkland Islands (flk), French Guiana (guf), Guyana (guy), Suriname (sur)
42	CRI	**Costa Rica**
43	GTM	**Guatemala**
44	HND	**Honduras**
45	NIC	**Nicaragua**
46	PAN	**Panama**
47	SLV	**El Salvador**
48	XCA	**Rest of Central America**
		Belize (blz)
49	DOM	**Dominican Republic**
50	JAM	**Jamaica**
51	PRI	**Puerto Rico**
52	TTO	**Trinidad & Tobago**
53	XCB	**Caribbean**
		Anguilla (aia), Antigua & Barbuda (atg), Aruba (abw), Bahamas (bhs), Barbados (brb), Cayman Islands (cym), Cuba (cub), Dominica (dma), Grenada (grd), Guadeloupe (glp), Haiti (hti), Martinique (mtq), Montserrat (msr), Netherlands Antilles (ant), Saint Kitts & Nevis (kna), Saint Lucia (lca), Saint Vincent & the Grenadines (vct), Turks and Caicos Islands (tca), British Virgin Islands (vgb), United States Virgin Islands (vir)

Table B.3: Regional dimension of the GTAP database (cont.)

54	AUT	**Austria**
55	BEL	**Belgium**
56	BGR	**Bulgaria**
57	CYP	**Cyprus**
58	CZE	**Czech Republic**
59	DNK	**Denmark**
60	EST	**Estonia**
61	FIN	**Finland**
62	FRA	**France**
63	DEU	**Germany**
64	GRC	**Greece**
65	HUN	**Hungary**
66	IRL	**Ireland**
67	ITA	**Italy**
68	LVA	**Latvia**
69	LTU	**Lithuania**
70	LUX	**Luxembourg**
71	MLT	**Malta**
72	NLD	**Netherlands**
73	POL	**Poland**
74	PRT	**Portugal**
75	ROU	**Romania**
76	SVK	**Slovakia**
77	SVN	**Slovenia**
78	ESP	**Spain**
79	SWE	**Sweden**
80	GBR	**United Kingdom**
81	NOR	**Norway**
82	CHE	**Switzerland**
83	XEF	**Rest of European Free Trade Area (EFTA)**
		Iceland (isl), Liechtenstein (lie)
84	ALB	**Albania**
85	BLR	**Belarus**
86	HRV	**Croatia**
87	RUS	**Russian Federation**
88	UKR	**Ukraine**
89	XEE	**Rest of Eastern Europe**
		Moldova (mda)
90	XER	**Rest of Europe**
		Andorra (and), Bosnia and Herzegovina (bih), Faroe Islands (fro), Gibraltar (gib), Macedonia (mkd, former Yugoslav Republic of), Monaco (mco), San Marino (smr), Serbia and Montenegro (scg)

Table B.4: Regional dimension of the GTAP database (cont.)

91	KAZ	**Kazakhstan**
92	KGZ	**Kyrgyz Republic**
93	TJK	**Tajikistan**
94	XSU	**Rest of Former Soviet Union**
		Turkmenistan (tkm), Uzbekistan (uzb)
95	ARM	**Armenia**
96	AZE	**Azerbaijan**
97	GEO	**Georgia**
98	BHR	**Bahrain**
99	IRN	**Iran**
100	ISR	**Israel**
101	JOR	**Jordan**
102	KWT	**Kuwait**
103	OMN	**Oman**
104	QAT	**Qatar**
105	SAU	**Saudi Arabia**
106	TUR	**Turkey**
107	ARE	**United Arab Emirates**
108	XWS	**Rest of Western Asia**
		Iraq (irq), Lebanon (lbn), West Bank and Gaza (pse), Syrian Arab Republic (syr), Republic of Yemen (yem)
109	EGY	**Egypt**
110	MAR	**Morocco**
111	TUN	**Tunisia**
112	XNF	**Rest of North Africa**
		Algeria (dza), Libya (lby)

Table B.5: Regional dimension of the GTAP database (cont.)

113	BEN	**Benin**
114	BFA	**Burkina Faso**
115	CMR	**Cameroon**
116	CIV	**Côte d'Ivoire**
117	GHA	**Ghana**
118	GIN	**Guinea**
119	NGA	**Nigeria**
120	SEN	**Senegal**
121	TGO	**Togo**
122	XWF	**Rest of Western Africa**
		Cape Verde (cpv), Gambia, The (gmb), Guinea-Bissau (gnb), Liberia (lbr), Mali (mli), Mauritania (mrt), Niger (ner), Saint Helena (shn), Sierra Leone (sle)
123	XCF	**Central Africa**
		Central African Republic (caf), Chad (tcd), Congo (cog), Equatorial Guinea (gnq), Gabon (gab), Sao Tome & Principe (stp)
124	XAC	**South-Central Africa**
		Angola (ago), Democratic Republic of the Congo (cod)
125	ETH	**Ethiopia**
126	KEN	**Kenya**
127	MDG	**Madagascar**
128	MWI	**Malawi**
129	MUS	**Mauritius**
130	MOZ	**Mozambique**
131	RWA	**Rwanda**
132	TZA	**Tanzania**
133	UGA	**Uganda**
134	ZMB	**Zambia**
135	ZWE	**Zimbabwe**
136	XEC	**Rest of Eastern Africa**
		Burundi (bdi), Comoros (com), Djibouti (dji), Eritrea (eri), Mayotte (myt), Réunion (reu), Seychelles Islands (syc), Somalia (som), Sudan (sdn)
137	BWA	**Botswana**
138	NAM	**Namibia**
139	ZAF	**South Africa**
140	XSC	**Rest of South African Customs Union**
		Lesotho (lso), Swaziland (swz)
141	XTW	**Rest of the World**
		Antarctica (ata), Bouvet Island (bvt), British Indian Ocean Territory (iot), French Southern Territories (atf)

Table B.6 provides the standard set of commodities (`COMM`) in the GTAP Data Base. In the standard database, these are the same as the set of activities (`ACTS`). The standard commodity subsets are:

- `MARG`, margin commodities: `OTP`, `WTP`, `ATP`
- `ERG`, energy commodities: `COA`, `OIL`, `GAS`, `P_C`, `ELY`, `GDT`
- `FUEL`, (fossil) fuel commodities: `COA`, `OIL`, `GAS`, `P_C`, `GDT`

Table B.6: Commodity dimension of the GTAP database

	Code	*Description*
1	PDR	Paddy rice
2	WHT	Wheat
3	GRO	Cereal grains nec
4	V_F	Vegetables, fruit, nuts
5	OSD	Oil seeds
6	C_B	Sugar cane, sugar beet
7	PFB	Plant-based fibers
8	OCR	Crops nec
9	CTL	Bovine cattle, sheep and goats, horses
10	OAP	Animal products nec
11	RMK	Raw milk
12	WOL	Wool, silk-worm cocoons
13	FRS	Forestry
14	FSH	Fishing
15	COA	Coal
16	OIL	Oil
17	GAS	Gas
18	OXT	Other Extraction (formerly omn Minerals nec)
19	CMT	Bovine meat products
20	OMT	Meat products nec
21	VOL	Vegetable oils and fats
22	MIL	Dairy products
23	PCR	Processed rice
24	SGR	Sugar
25	OFD	Food products nec
26	B_T	Beverages and tobacco products
27	TEX	Textiles
28	WAP	Wearing apparel
29	LEA	Leather products
30	LUM	Wood products
31	PPP	Paper products, publishing
32	P_C	Petroleum, coal products
33	CHM	Chemical products
34	BPH	Basic pharmaceutical products
35	RPP	Rubber and plastic products

Table B.7: Commodity dimension of the GTAP database (cont.)

36	NMM	Mineral products nec
37	I_S	Ferrous metals
38	NFM	Metals nec
39	FMP	Metal products
40	ELE	Computer, electronic and optical products
41	EEQ	Electrical equipment
42	OME	Machinery and equipment nec
43	MVH	Motor vehicles and parts
44	OTN	Transport equipment nec
45	OMF	Manufactures nec
46	ELY	Electricity
47	GDT	Gas manufacture, distribution
48	WTR	Water
49	CNS	Construction
50	TRD	Trade
51	AFS	Accommodation, Food and service activities
52	OTP	Transport nec
53	WTP	Water transport
54	ATP	Air transport
55	WHS	Warehousing and support activities
56	CMN	Communication
57	OFI	Financial services nec
58	INS	Insurance (formerly isr)
59	RSA	Real estate activities
60	OBS	Business services nec
61	ROS	Recreational and other services
62	OSG	Public Administration and defense
63	EDU	Education
64	HHT	Human health and social work activities
65	DWE	Dwellings

The power-version of the GTAP database splits the standard electricity sector (`'ELY'`) into 12 electricity-based activities—11 of which are different power technologies with differentiated cost structures and 1 activity for transmission and distribution. The database assumes full diagonality of the power structure 'make' matrix. A typical model implementation is likely to keep the differentiated cost structures but collapse demand to a single electricity commodity.[1]

Table B.8: Additional dimensions of the power database

	Code	*Description*
1	TND	Electricity transmission and distribution
2	NUCLEARBL	Nuclear power
3	COALBL	Coal power baseload
4	GASBL	Gas power baseload
5	WINDBL	Wind power
6	HYDROBL	Hydro power baseload
7	OILBL	Oil power baseload
8	OTHERBL	Other baseload
9	GASP	Gas power peakload
10	HYDROP	Hydro power peakload
11	OILP	Oil power peakload
12	SOLARP	Solar power

The standard version of GTAP has 8 endowments or factors of production—of which 5 are labor types. The first three labor types in Table B.9 are typically associated with *unskilled* labor and the remaining two would therefore be designated *skilled* labor.[2] It should be noted that in the default configuration, land payments are only attributed in the agricultural sectors—both crops and livestock—but not forestry. Natural resource payments are available for forestry (`frs`), fisheries (`fsh`), coal mining (`coa`), oil and gas extraction (`oil` and `gas`) and other mining extraction (`oxt`).

Table B.9: GTAP endowments

	Code	*Description*
1	TECH_ASPROS	Technical and professional workers
2	CLERKS	Clerical workers
3	SERVICE_SHOP	Service shop
4	OFF_MGR_PROS	Management
5	AG_OTHLOWSK	Agriculture and other low-skill workers
6	CAPITAL	Capital
7	LAND	Land
8	NATLRES	Natural resources

Table B.10 provides the definitions for the greenhouse (GHG) and non-greenhouse gases. The set `EM` incorporates all air emissions. The set `EMN` incorporates all air emissions with the exception of CO_2. The set `GHG` includes the four greenhouse gases (CO_2, CH_4, N_2O and `FGAS`). The set `NCO2` represents the greenhouse gases except CO_2. The set `NGHG` includes all non-greenhouse gases. The emissions database also contains a set linked to the Intergovernmental Panel on Climate Change

[1] The 12 power activities are added to the `ERG` subset.

[2] Walmsley and Carrico (2016).

(IPCC) assessment reports. The set is named `IPCC_REP`. The latest version of this set contains `AR2, AR4 & AR5`.

Table B.10: Air emissions

	Code	*Description*
1	CO2	Carbon dioxide
2	CH4	Methane
3	N2O	Nitrous oxide
4	FGAS	Fluorinated gases
5	BC	Black carbon
6	CO	Carbon monoxide
7	NH3	Ammonia
8	NMVOC	Non-methane volatile organic compounds
9	NOX	Nitrogen oxides
10	OC	Organic carbon
11	PM10	Particulate matter 10
12	PM2_5	Particulate matter 2.5
13	SO2	Sulfur dioxide

The emissions database contains land-based greenhouse gas emissions. The following two tables provide the sets used for these emissions. The first is the broad categorization of land, and the second links it to specific types.

Table B.11: Emissions linked to land-use types

	Code	*Description*
1	CrpLand	Crop land
2	GrsLand	Grass land
3	FrsLand	Forest land
4	BrnBiom	Burning biomass

Table B.12: Emissions linked to land-use sub-types

	Code	*Description*
1	CrpSoil	Crop soil
2	GrsSoil	Grass soil
3	OrgSoil	Organic soil
4	FrsLand	Forest land
5	FrsConv	Forest conversion
6	TropFrs	Tropical forest
7	OthrFrs	Other forest

Bibliography

Chepeliev, M. 2020. "Development of the Non-CO2 GHG Emissions Database for the GTAP Data Base Version 10A." Global Trade Analysis Project (GTAP), Department of Agricultural Economics, Purdue University, West Lafayette, IN, GTAP Research Memorandum No. 32. https://www.gtap.agecon.purdue.edu/resources/res_display.asp?RecordID=5993.

Hänsel, M.C., M.A. Drupp, D.J.A. Johansson, F. Nesje, C. Azar, M.C. Freeman, B. Groom, and T. Sterner. 2020. "Climate economics support for the UN climate targets." *Nature Climate Change*, 10: 781–789. doi:10.1038/s41558-020-0833-x.

Hartin, C.A., P. Patel, A. Schwarber, R.P. Link, and B. Bond-Lamberty. 2015. "A simple object-oriented and open-source model for scientific and policy analyses of the global climate system—Hector v1.0." *Geoscientific Model Development*, 8(4): 939–955. doi:10.5194/gmd-8-939-2015.

Joos, F., R. Roth, J.S. Fuglestvedt, G.P. Peters, I.G. Enting, W. von Bloh, V. Brovkin, E.J. Burke, M. Eby, N.R. Edwards, T. Friedrich, T.L. Frölicher, P.R. Halloran, P.B. Holden, C. Jones, T. Kleinen, F.T. Mackenzie, K. Matsumoto, M. Meinshausen, G. Plattner, A. Reisinger, J. Segschneider, G. Shaffer, M. Steinacher, K. Strassmann, K. Tanaka, A. Timmermann, and A.J. Weaver. 2013. "Carbon dioxide and climate impulse response functions for the computation of greenhouse gas metrics: a multi-model analysis." *Atmospheric Chemistry and Physics*, 13(5): 2793–2825. doi:10.5194/acp-13-2793-2013.

Leach, N.J., S. Jenkins, Z. Nicholls, C.J. Smith, J. Lynch, M. Cain, T. Walsh, B. Wu, J. Tsutsui, and M.R. Allen. 2020. "FaIRv2.0.0: a generalised impulse-response model for climate uncertainty and future scenario exploration." *Geoscientific Model Development Discussions*, 2020: 1–48. doi:10.5194/gmd-2020-390.

Manne, A., R. Mendelsohn, and R. Richels. 1995. "MERGE: A model for evaluating regional and global effects of GHG reduction policies." *Energy Policy*, 23(1): 17–34. doi:10.1016/0301-4215(95)90763-W.

Meinshausen, M., T.M.L. Wigley, and S.C.B. Raper. 2011. "Emulating coupled atmosphere-ocean and carbon cycle models with a simpler model, MAGICC6—Part 1: Model description and calibration." *Atmospheric Chemistry and Physics*, 11(4): 1417–1456. doi:10.5194/acp-11-1417-2011.

Millar, R.J., Z.R. Nicholls, P. Friedlingstein, and M.R. Allen. 2017. "A modified impulse-response representation of the global near-surface air temperature and atmospheric concentration response to carbon dioxide emissions." *Atmospheric Chemistry and Physics*, 17(11): 7213–7228. doi:10.5194/acp-17-7213-2017.

Nordhaus, W.D. 2016. "Projections and Uncertainties About Climate Change in an Era of Minimal Climate Policies." National Bureau of Economic Research, Working Paper No. 22933, December. doi:10.3386/w22933.

O'Neill, B.C., E. Kriegler, K.L. Ebi, E. Kemp-Benedict, K. Riahi, D.S. Rothman, B.J. van Ruijven, D.P. van Vuuren, J. Birkmann, K. Kok, M. Levy, and W. Solecki. 2015. "The roads ahead: Narratives for shared socioeconomic pathways describing world futures in the 21st century." *Global Environmental Change*, pp. –. doi:http://dx.doi.org/10.1016/j.gloenvcha.2015.01.004.

Riahi, K., D.P. van Vuuren, E. Kriegler, J. Edmonds, B.C. O'Neill, S. Fujimori, N. Bauer, K. Calvin, R. Dellink, O. Fricko, W. Lutz, A. Popp, J.C. Cuaresma, S. KC, M. Leimbach, L. Jiang, T. Kram, S. Rao, J. Emmerling, K. Ebi, T. Hasegawa, P. Havlík, F. Humpenöder, L.A. Da Silva, S. Smith, E. Stehfest, V. Bosetti, J. Eom, D. Gernaat, T. Masui, J. Rogelj, J. Strefler, L. Drouet, V. Krey, G. Luderer, M. Harmsen, K. Takahashi, L. Baumstark, J.C. Doelman, M. Kainuma, Z. Klimont, G. Marangoni, H. Lotze-Campen, M. Obersteiner, A. Tabeau, and M. Tavoni. 2016. "The Shared Socioeconomic Pathways and their energy, land use, and greenhouse gas emissions implications: An overview." *Global Environmental Change*, pp. –. doi:http://dx.doi.org/10.1016/j.gloenvcha.2016.05.009.

Smith, C.J., P.M. Forster, M. Allen, N. Leach, R.J. Millar, G.A. Passerello, and L.A. Regayre. 2018. "FAIR v1.3: a simple emissions-based impulse response and carbon cycle model." *Geoscientific Model Development*, 11(6): 2273–2297. doi:10.5194/gmd-11-2273-2018.

U.S. EPA. 2019. "Global Non-CO2 Greenhouse Gas Emission Projections & Mitigation: 1990-2050." United States Environmental Protection Agency, Office of Atmospheric Programs (6207A), Washington, DC 20005, Report No. EPA-430-R-19-010. https://www.epa.gov/globalmitigation-non-co2-greenhouse-gases.

van der Mensbrugghe, D. 2019. "The Environmental Impact and Sustainability Applied General Equilibrium (ENVISAGE) Model. Version 10.01." Center for Global Trade Analysis (GTAP), Department of Agricultural Economics, Purdue University, West Lafayette, IN, Unpublished manuscript. https://mygeohub.org/groups/gtap/envisage-docs.

Walmsley, T., and C. Carrico. 2016. "Disaggregating Labor Payments." In *Global Trade, Assistance, and Production: The GTAP 9 Data Base*, edited by B. G. Narayanan, A. Aguiar, and R. McDougall. Department of Agricultural Economics, Purdue University, West Lafayette, IN, chap. 12. https://www.gtap.agecon.purdue.edu/resources/res_display.asp?RecordID=4867.

Weyant, J.P., F.C. de la Chesnaye, and G.J. Blanford. 2006. "Overview of EMF-21: Multigas Mitigation and Climate Policy." *The Energy Journal*, 27: 1–32. http://www.jstor.org/stable/23297073.